

A Pulsed Electric Field Enhances Cutaneous Delivery of Methylene Blue in Excised Full-Thickness Porcine Skin

Patricia G. Johnson, Stephen A. Gallo, Sek Wen Hui, and Allan R. Oseroff*

Departments of Molecular and Cellular Biophysics and *Dermatology, Roswell Park Cancer Institute, Buffalo, New York, U.S.A.

We used electric pulses to permeabilize porcine stratum corneum and demonstrate enhanced epidermal transport of methylene blue, a water-soluble cationic dye. Electrodes were placed on the outer surface of excised full-thickness porcine skin, and methylene blue was applied to the skin beneath the positive electrode; 1 ms pulses of up to 240 V were delivered at frequencies of 20–100 Hz for up to 30 min. The amount of dye in a skin sample was determined from absorbance spectra of dissolved punch biopsy sections. Penetration depth and concentration of the dye were measured with light and fluorescence microscopy of cryosections. At an electric exposure dose VT (applied voltage × frequency × pulse width × treatment duration) of about 4700 Vs, there is a threshold for efficient drug delivery. Increasing the

applied voltage or field application time resulted in increased dye penetration. Transport induced by electric pulses was more than an order of magnitude greater than that seen following iontophoresis. We believe that the enhanced cutaneous delivery of methylene blue is due to a combination of *de novo* permeabilization of the stratum corneum by electric pulses, passive diffusion through the permeabilization sites, and electrophoretic and electroosmotic transport by the electric pulses. Pulsed electric fields may have important applications for drug delivery in a variety of fields where topical drug delivery is a goal. Key words: electroporation/iontophoresis/photodynamic therapy/topical administration. *J Invest Dermatol* 111:457–463, 1998

Topical drug administration has potential advantages over oral, injection, or intravenous drug delivery. These advantages include convenience, noninvasiveness, minimal trauma induction, and avoidance of “first-pass” degradation or metabolism in the gastrointestinal tract or liver. Tightly localized administration is possible, and systemic delivery can be achieved through absorption by the dermal blood supply. The main barrier to cutaneous or transcutaneous drug delivery is the impermeability of the stratum corneum (SC), the outermost layer of the skin (Scheuplein and Bronaugh, 1983). If the integrity of the SC is disrupted, the barrier to molecular transit may be greatly reduced.

Cutaneous absorption may be increased by removal of the SC by tape-stripping or dermabrasion, excimer laser ablation (Jacques *et al*, 1987), or vehicle (solvent-carrier) optimization and the use of penetration enhancers like dimethyl sulfoxide, oleic acid, and alcohols (Singh and Singh, 1993; Berti and Lipsky, 1995). Disruption of the SC also can be achieved by electroporation, i.e., the creation of penetration sites by an electric field. These penetration sites, although not yet well characterized, are thought to be aqueous pores of nanometer size with lifetimes from milliseconds to seconds (Chang, 1992). Ions and molecules move through induced gaps of the SC by diffusion and electromotive or electroosmotic transport (Edwards and Langer, 1994; Chizmadzhev *et al*, 1995; Edwards *et al*, 1995). Electroporation differs

from iontophoresis – the increased migration of ions or charged molecules through the skin when an electrical potential gradient is applied. The primary transdermal iontophoretic route seems to be appendageal or intercellular through pre-existing pathways (Edwards and Langer, 1994; Lee *et al*, 1996), or as a result of low-voltage (<5 V) induced permeabilization of appendageal bilayers (Chizmadzhev *et al*, 1998). A third form of electroenhanced drug delivery, electrochemotherapy (Mir *et al*, 1995), refers to the local delivery of electric pulses across a tumor following systemic drug administration, and usually does not involve cutaneous or transcutaneous delivery.

Studies have described electroporation-enhanced transport of molecules across skin, using heat-stripped SC or epidermis, mounted between flow-through chambers (Bommannan *et al*, 1994; Prausnitz *et al*, 1995; Vanbever and Pr eat, 1995; Pliquett *et al*, 1996). Animal *in vivo* work has been reported using murine models to study the electroporative delivery of drugs (Prausnitz *et al*, 1993), microspheres (Hofmann *et al*, 1995), and DNA (Titomirov *et al*, 1991). Riviere’s group has developed and used an isolated perfused porcine skin flap as an *in vitro* model for drug transport studies (Riviere and Monteiro-Riviere, 1991; Riviere *et al*, 1995). We chose pig skin as a model because its structure and characteristics closely approximate those of human skin (Bronaugh *et al*, 1982; Ferry *et al*, 1995; Steinstrasser and Merkle, 1995). To simulate *in vivo* conditions we used full-thickness skin with two electrodes attached to the skin surface; short, high voltage pulses were used to permeabilize the SC.

Topical drug delivery has the potential for use in many applications, including the localized delivery of anesthetics, antibiotics, steroids, and chemotherapeutic agents. This technique should have particular advantages in the field of photodynamic therapy, where localized rather than systemic administration is a goal. We used the phenothiazinium dye methylene blue (MB) in these studies because its color allows visual observation of its location, its absorbance and fluorescence

Manuscript received January 31, 1998; revised February 12, 1998; accepted for publication May 13, 1998.

Reprint requests to: Dr. Patricia G. Johnson, Department of Molecular and Cellular Biophysics, Roswell Park Cancer Institute, Elm and Carlton Streets, Buffalo, New York 14263.

Abbreviations: MB, methylene blue; SC, stratum corneum; VT, electrical exposure dose.

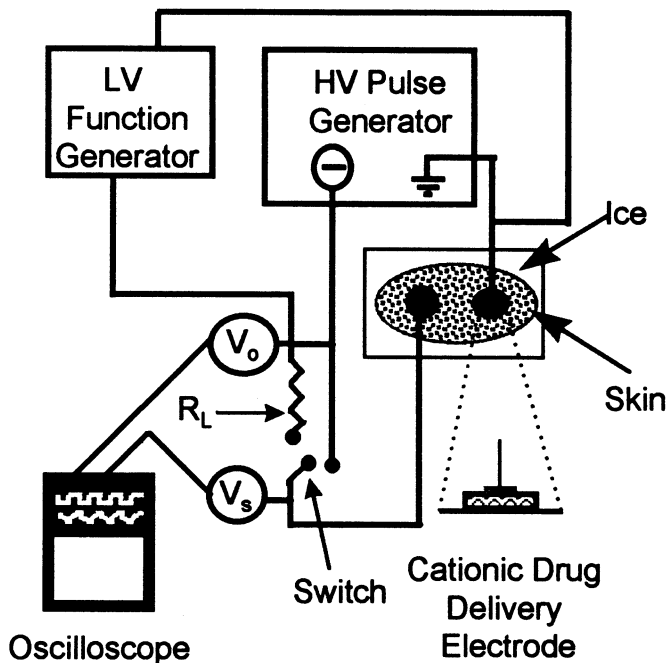


Figure 1. Schematic diagram of the system used to monitor skin resistance and to deliver electric pulses.

properties permit spectroscopic detection, and its cationic nature serves as a model for a number of photosensitizers currently under investigation.¹

MATERIALS AND METHODS

Skin Belly skin from domestic pigs was obtained from a local abattoir and a cardiopulmonary research laboratory. Fresh samples, stored on ice, were used within 48 h. Full-thickness 10 × 20 cm sections were washed and shaved with electric clippers. Skin was placed, dermal side down, on Saran Wrap on ice. Each skin section was typically used for 3–6 measurements; both electrodes were placed on a previously unused region before resistance measurements or pulsing began.

Experimental set-up (Fig 1) Ag-AgCl electrodes (diameter = 8 mm, In Vivo Metric, Healdsburg, CA) were attached (5 cm apart) to the skin with adhesive electrode washers (In Vivo Metric); Sigma Gel Saline electrode gel (Parker Laboratories, Orange, NJ) was used to ensure a good electrical connection. For drug delivery, a small piece of cotton soaked with 200 μ l of MB (Fisher Scientific, Fairlawn, NJ, 1% in ddH₂O, 0.03 M) was placed in the cavity of the active electrode.

Pre- and postpulse skin resistance was measured using continuous low voltage (300 mV) 1000 Hz bipolar square waves from a Dynascan Model 3300 pulse generator (Chicago, IL). A load resistor (4.7 k Ω) was placed in series with the skin, and the voltage drop across the whole circuit (V_o) or just across the skin (V_s) was measured by a recording digital oscilloscope (Fluke 99 Scopemeter Series II, Everett, WA). Skin resistance (in k Ω) was approximated from the formula $R_s = (V_s \times R_L) / (V_o - V_s)$, where R_s is the skin resistance and R_L is the load resistor. A skin sample was used only if the pretreatment resistance equaled 5 k Ω or more.

Electroporation was carried out using a pulse generator (Model 345, Velonex, Santa Clara, CA) delivering multiple unipolar square pulses up to 240 V, at frequencies of 20–100 Hz with a 1 ms pulse width. The electric exposure dose VT (in Vs) was calculated as $V \times f \times \tau \times t$ (Liang *et al*, 1988) where V is the applied voltage, T = $f \times \tau \times t$ is the field application time, f is the frequency (Hz), τ is the pulse width (ms), and t is the treatment duration (s). Iontophoresis was performed using 5 V direct current (0.19 and 0.32 mA per cm² for 30 and 60 min, respectively) generated by a Hewlett-Packard 6236 A Triple Output Power Supply.

Optical density of dissolved-sample supernatant After treatment the skin was rinsed to remove superficial dye. Full-thickness 5 mm punch biopsy samples (mean weight 38.6 mg) were dissolved overnight in 1 ml Solvable (Packard Instrument, Meriden, CT) at 37°C. Solutions were centrifuged, and absorbance spectra of the supernatant fractions were recorded. This method of dye quantitation is a modification of the technique reported by Bellnier *et al* (1997) and Lilge *et al* (1997), whereby we used absorbance rather than fluorescence spectroscopy to monitor drug levels. The extinction coefficient of MB in Solvable ($\approx 30,000$ per cm per M at $\lambda = 598$ –600 nm) was determined from an absorbance *versus* concentration plot (data not shown). Transport across the skin surface was calculated as μ g dye per cm². Average flux (μ g per cm² per min) was calculated as the amount of dye in μ g transported across an area of 0.196 cm² divided by t, the treatment duration. Data and error are presented as mean \pm SD unless stated otherwise.

Light microscopy Full-thickness 1 cm² biopsies were embedded in Tissue-Tek O.C.T. compound (Miles, Elkhart, IN), and frozen in liquid nitrogen. Photomicrographs of cryostat sections (10 μ m) perpendicular to the skin surface were prepared. Also, images were collected with a Dage MTI CCD72 camera (Dage-MTI, Michigan City, IN) with a 615 nm long-pass filter, and processed with Image 1 software (Universal Imaging, West Chester, PA). The dye was quantitated by measuring the transmission at wavelengths > 615 nm for each of 300 pixels along a line normal to the skin surface. Pixel number was converted to depth in μ m by calibration with a section of known dimensions; pixel size = 0.20 μ m² (0.45 × 0.45 μ m).

Fluorescence microscopy Intensified digital fluorescence microscopy was performed with a Zeiss Axiovert 35 inverted epifluorescence microscope with a 200 W mercury arc lamp for illumination. Images were obtained with a Dage MTI CCD72 camera and GenII Sys intensifier. MB fluorescence was excited with 630 nm light² from a 5 W argon laser (Spectra-Physics 164) pumping a Spectra-Physics Model 375 dye laser using DCM dye (Exciton, Dayton, OH), tuned to the appropriate wavelength by a birefringence filter, and was detected using a 660 nm long-pass filter (Tuite and Kelly, 1993). Quantitation of fluorescence intensity was made by averaging across a 20-pixel wide zone, at each of 300 pixels along a band normal to the skin surface; pixel size = 0.20 μ m².

RESULTS

MB blue staining depended on electrical conditions Following MB application, skin was observed at 20 \times magnification under a stereo microscope. With no electric field, very little staining of the skin surface was seen, with some MB concentration in skin creases. After iontophoresis (5 V, 0.3 mA per cm², 60 min, VT = 9000 Vs), less than 10% of the skin surface was stained dark blue in a punctate pattern, with the heaviest staining in follicles and around hair shafts. Following electroporation (240 V, 40 Hz, 1 ms, 10–30 min, 5750–17,280 Vs) there was no follicular accentuation, and the entire skin surface was stained blue (data not shown).

MB penetration into the epidermis was seen in cryosections (Fig 2) Under passive diffusion conditions, no MB was observed (Fig 2a). With pulsing at 3600 Vs the dye entered the SC (Fig 2b), whereas at a higher dose of 7200 Vs MB penetration into both the SC and the epidermis was seen (Fig 2c). Pulsing at 14,400 Vs produced migration of MB through the SC, a high concentration of dye in the epidermis, and the appearance of some dye in the dermis (Fig 2d). The dark bands seen at the SC surface in Fig 2(b, d) are not due to the presence of MB, but are dark areas that appear to be artifacts due to density differences in the inhomogeneous skin. (Similar darker bands can be seen at the edges of the SC in Fig 2a.)

MB penetration depends on electric exposure dose, particularly field application time and voltage The amount of MB delivered to the skin increased with field application time T (Table I) when voltage, frequency, and pulse width were held constant. The rate of increase of dye penetration for the mean absorbance values as a function of T (Fig 3a), was fit by a sigmoidal relationship³ with a correlation coefficient $r^2 = 0.956$.⁴ When VT was held constant at 8640 Vs, the amount of MB recovered increased exponentially⁵ as the voltage increased (Fig 3b, $r^2 = 0.999$). At a constant VT = 7200, penetration remained constant at frequencies of 20–60 Hz (124 ± 97 μ g per cm²,

¹Johnson PG, Rideout DA, Camacho SH, Oseroff AR: Photodynamic therapy using Victoria Blue-BO analogs: *in vivo* toxicity and efficacy toward murine colo-26 and human FaDu tumors in mice. *Photochem Photobiol* 6359S:31S, 1994 (abstr.)

²Aqueous MB has a broad absorbance band at 598–640 nm.

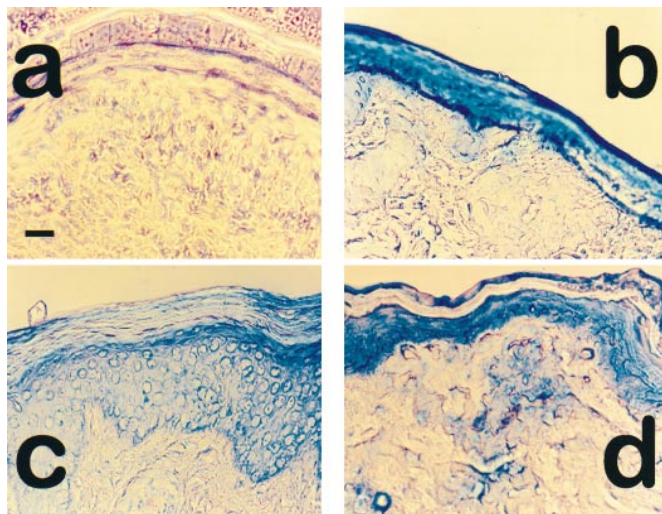


Figure 2. Visualization of MB penetration. Photomicrographs (light microscopy, 40 \times) of frozen section biopsies of porcine skin following MB application: (a) Control, MB applied to the skin surface for 30 min, no pulse; (b) 200 V, 10 Hz, $\tau = 1$ ms, 30 min, 3600 Vs; (c) 100 V, 40 Hz, $\tau = 1$ ms, 30 min, 7200 Vs; (d) 200 V, 40 Hz, $\tau = 1$ ms, 30 min, 14,400 Vs. Scale bar: 50 μ m.

$n = 14$). At frequencies ≥ 70 Hz, MB penetration increased significantly (317 ± 163 μ g per cm^2 , $n = 9$, $p < 0.002$, Fig 3c); however, at the higher frequencies severe skin damage (e.g., blistering) was seen.

As VT increased from 576 to 17,280 Vs, transport increased from ≈ 10 to 50 μ g per cm^2 (Table I). MB average flux ranged from 2 to 10 μ g per cm^2 per min, with a mean value of 3.5 ± 2.3 ($n = 45$). No correlation between flux and exposure time (or VT) was seen.

MB delivered by electroporation showed much greater penetration than dye delivered by iontophoresis or passive diffusion Following iontophoresis (5 V, 0.19 mA per cm^2 , 30 min, VT = 9000 Vs) or passive diffusion, no MB was detectable in the samples (i.e., the optical density was < 0.01 , no greater than background values). At 0.32 mA per cm^2 (5 V, 60 min, VT = 18,000 Vs), virtually no MB penetration into the SC was seen with microscopic examination of cryosections.

Some of the changes induced by electroporation appeared to persist after the electric pulses had stopped. Electroporation was carried out (5760 Vs, 240 V, 40 Hz, 10 min) with no MB present. At various times (0–30 min) following the conclusion of pulsing, MB was applied to the skin for 30 min. At all postpulse application times, penetration was significantly greater than with either 30 min passive diffusion with no preapplication pulsing, or iontophoresis ($p < 0.05$, Table I). MB penetration was also significantly higher when the drug was applied immediately after pulsing than at 10, 20, or 30 min after pulsing. No correlation was seen with MB levels and postpulse application times > 0 .

Absorbance measurements of MB tissue levels correlate well with light and fluorescence microscopy data Light microscopy data (Fig 4a) show very little MB present in the biopsy section under no-pulse conditions. As VT increases, there is increased penetration, reflected by the greater total amount of dye present in the section (area under the curve) and by the increased depth at which the maximum concentration appears. Similar behavior is seen from the

³ $Y = OD_{\min} + (OD_{\max} - OD_{\min}) / [1 + e^{(T_{50} - x)/dx}]$, where T_{50} , the value of X at $Y = 50\%$, is 19.5 ± 1.3 (SD) s (95% confidence interval, 11.2–27.9 s).

⁴Specimens were held on ice during treatment. This was done primarily so that degradation of the skin sample would be slowed. The actual surface temperature of the tissue was 10°C ($\pm 0.5^\circ\text{C}$). In order to validate our studies carried out on ice, experiments were conducted using samples maintained at room temperature. For room temperature skin, $T_{50} = 18.2$, a value within one SD of the value seen for the cooled samples.

⁵The data are well fit by the expression $\ln(\text{MB}) = 0.0171x - 3.53$.

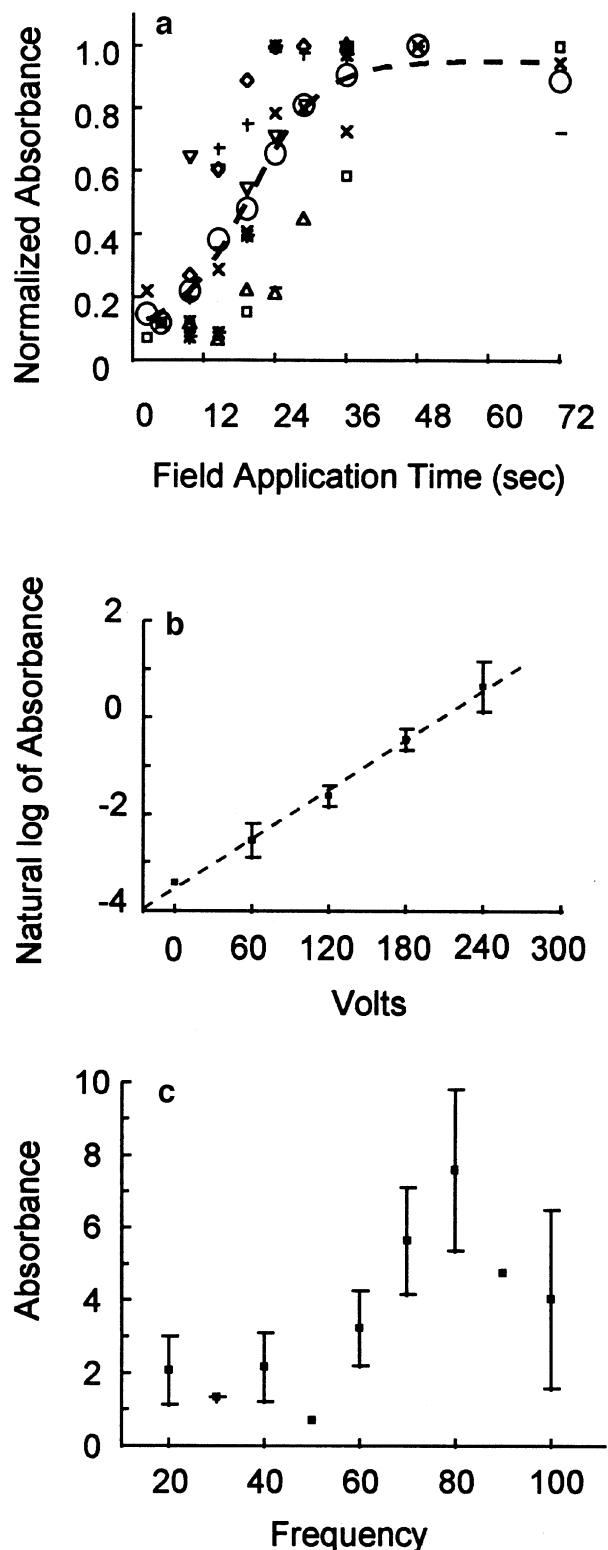


Figure 3. Total penetration of MB in a 5 mm punch biopsy, measured as the absorbance of drug in Solvable supernatant. Penetration as a function of the following. (a) Field application time: all samples were pulsed at a constant voltage (240 V), frequency (40 Hz), and pulse width (1 ms) for 1–30 min. Various symbols represent individual experiments; for each experiment, all absorbance values were normalized to the maximum optical density recorded for that experiment; \circ , mean values; ---, sigmoidal fit. (b) Voltage: all samples (8640 Vs) were pulsed at a constant frequency (40 Hz) and pulse width (1 ms) at 60–240 V for 60–15 min; plotted as natural log of absorbance versus voltage; ---, linear fit of exponential relationship. (c) Frequency: samples were pulsed at a constant voltage and pulse width at frequencies of 20–100 Hz for 6–30 min; mean value (\pm SD)

Table I. Quantitation of delivery of MB^a

Field application time (s) (treatment) (duration in min)	VT (Vs)	Mean OD ^{b,c}	n ^d	SD	mg MB per g tissue ^e	Transport (µg per cm ²)	Average flux (µg per cm ² per min)	Average flux (µg per cm ² per h)
2.4 (1)	576	0.181	2	0.16	0.050	9.8	9.84	591
4.8 (2)	1152	0.135	2	0.04	0.037	7.4	3.68	221
9.6 (4)	2304	0.173	6	0.07	0.048	9.4	2.36	142
14.4 (6)	3456	0.255	6	0.13	0.071	13.9	2.32	139
19.2 (8)	4608	0.414	6	0.20	0.114	22.5	2.82	169
24.0 (10)	5760	0.647	6	0.44	0.179	35.2	3.52	211
28.8 (12)	6912	0.807	4	0.23	0.223	43.9	3.66	220
36.0 (15)	8640	0.930	7	0.55	0.257	50.6	3.38	203
48.0 (20)	11520	0.827	3	0.46	0.229	45.0	2.25	135
72.0 (30)	17280	0.893	3	0.40	0.247	48.6	1.62	97
MEAN (± SD)							3.54 (±2.3)	213 (±139)
30 min (postpulse dye application)	5760	0.044	20	0.017		2.4	0.08	4.8
30 min (passive diffusion)	0	0.018	11	0.005		1.0	0.03	1.8
30 min (iontophoresis)	9000	ND ^f					< 0.03	< 1.8

^aAll samples were pulsed at a constant voltage (240 V), frequency (40 Hz), and pulse width (1 ms), for 1–30 min.

^bOptical density was obtained from absorbance spectra of the supernatant from Solvable dissolved tissue samples.

^cAt the 0.05 level, the means are significantly different (ANOVA analysis).

^dn, number of experiments.

^eThe amount of dye in the sample was estimated using an extinction coefficient $\epsilon = 30,000$ per M per cm (1 cm path width) and a molecular weight of 320. Biopsy weight = 38.6 (± 3.3) mg.

^fNot detectable.

MB fluorescence emission assay (Fig 4b). There is a small MB peak seen with VT = 0 in the first 10–20 µm, reflective of localization at the surface of the SC. With increasing VT there is increased dye penetration. Penetration was quantitated by integrating the area under each curve. In a plot of the area versus VT (Fig 5) for both fluorescence and transmittance data, similar behavior is noted: an increase in area as a function of increasing VT. Fluorescence data reflect the greater sensitivity of that method, as seen by the earlier rise in penetration – between 900 and 1500 Vs – as compared with the optical density data where the rise is not seen until the electrical exposure dose exceeds 3600 Vs. Because of the inherent sensitivity of fluorescence detection, this method is particularly effective with low concentrations of the dye, whereas optical density assays are useful in the higher concentration ranges.

Finally, we see in Fig 6 that the two methods of MB quantitation using optical density as a criterion, i.e., concentration (via absorbance) in Solvable supernatant and image analyses using transmitted light, yield very similar behavior trends.

DISCUSSION

Epidermal delivery of MB is enhanced by the application of electric pulses. Even at low electric exposure doses, MB transport was orders of magnitude greater than that seen using iontophoresis or passive diffusion. Enhanced MB penetration was also observed when the drug was applied to the skin after pulsing. Good agreement among the various assays was found.

When pulsed at a constant voltage, frequency, and pulse width, transport increases as the field application time or electrical exposure dose increases (Fig 3a, Table I). This relationship was best fit by a sigmoidal curve. The fit was empirically, and not theoretically, derived, and reflects the plateau in MB penetration seen in our system at field application times > 24 s (VT = 5760). At electric exposure doses above that level, MB penetration may be somewhat impeded by tissue saturation. More significantly, depletion of the drug in the donor electrode undoubtedly contributes to the plateau.

The increase of MB transport shows a step jump at a threshold dose between 3500 and 5800 Vs. If the sizes of pores are related to the dose, a step jump might be expected to appear when the average pore size becomes large enough to accommodate the molecule in question, and diffusion and electromotive transport through long-term openings begins to contribute to the total transport.

The difference in thresholds for resistance drop (Gallo *et al*, 1997) and MB penetration probably reflect the criteria of different pore size requirements for each respective case. Molecules of sizes smaller than the pores created by a given dose are free to diffuse through the permeabilized barrier in the absence of pulses, in addition to those molecules driven through these pores during the pulses. The threshold of about 4700 Vs for efficient MB transport is considerably higher than that for small ion conductance in resistance measurements (200 Vs), as expected, given the larger size of the MB molecule.

At plateau pulsing conditions (T = 36 s, VT = 8640 Vs), transport increases exponentially as a function of pulse voltage (Fig 3b). This exponential voltage dependence for transport differs from our observation of changes in the skin's electrical resistance as a function of pulse voltage (Gallo *et al*, 1997). In that instance we found that long-term electrical resistance of the skin decreased as the voltage of the pulse increased, but this voltage-dependent decrease in skin resistance reached a plateau at about a 75% drop in resistance. Yet MB penetration continues to rise as the voltage increases (Fig 3b). This discrepancy results from the fact that different aspects of the electro-transport phenomenon are being monitored. Resistance measurements reflect permeabilization of the SC, implying the creation or enlargement of openings through the SC through which electrolytes flow. As resistance drops, voltage is redistributed across the SC and other layers, reducing the voltage gradient across the SC and reducing the probability that additional poration will occur. In transport measurements, molecular flow continues to increase as the voltage increases, due to the driving electrophoretic force. We assume that the amount of MB transport is proportional to the probability of pore formation as a consequence of the applied pulses, and is a function of the applied electric energy of the pulse train. The electric energy of the pulse may be expressed as V^2T/R , where R is the electrical resistance between electrodes. For simplicity's sake we assume R to be constant throughout the pulse train application. The probability of the applied energy reaching the pore formation energy threshold $\epsilon_0 = (V_0^2T)/R$ is given by the Boltzmann equation $P = e^{(\epsilon - \epsilon_0)/kT}$, where k is the Boltzmann constant and T' is the absolute temperature. Because the experimental data in Fig 3(b) were collected with VT = K, where K is constant, then $T = K/V$. The Boltzmann equation may be written as $P = e^{(V - V_0)C}$, where C is a constant for a given temperature. Plotting [MB] against V, under the constraint of constant VT, will result in an exponential dependence of [MB] on V.

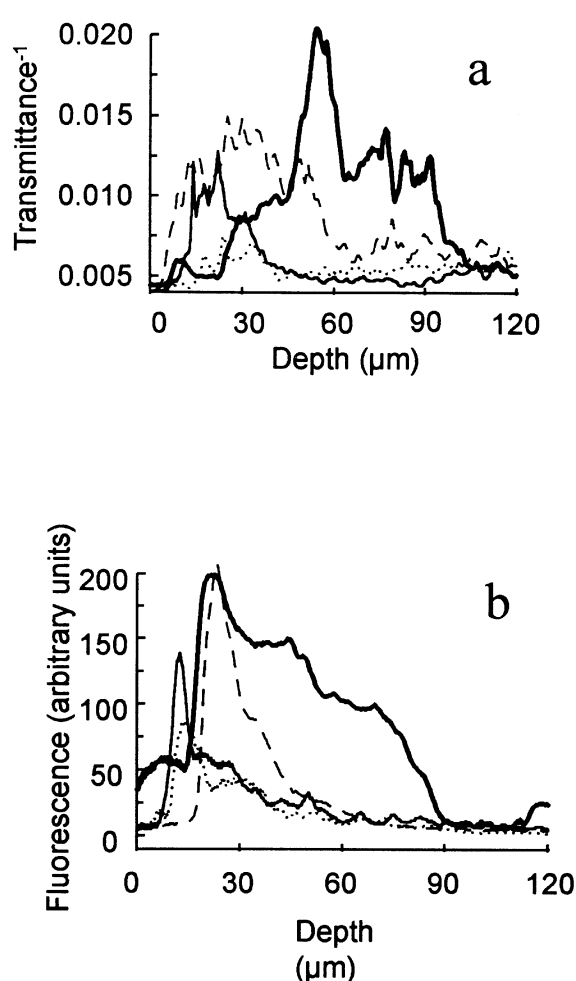


Figure 4. Concentration of MB versus penetration depth. (a) Concentration as measured by image analyses of transmitted light (>615 nm): \dots , no pulse; $—$, 1800 Vs, 10 Hz, 100 V; $- - -$, 18,000 Vs, 100 V, 100 Hz; \blacksquare , 45,000 Vs, 250 V, 100 Hz. All at $\tau = 1$ ms for 30 min. (b) Concentration as measured by fluorescence emission (630 nm excitation, detected using a 660 nm long-pass filter): \dots , no pulse; $—$, 360 Vs, 20 V, 10 Hz; $- - -$, 900 Vs, 50 V, 10 Hz; \blacksquare , 1800 Vs, 100 V, 10 Hz. All at $\tau = 1$ ms for 30 min.

MB penetration does not depend on the pulse frequency between 20 and 60 Hz. Similarly, we have previously shown that the maximum decrease in skin resistance is reached at a frequency of 30–50 Hz (Gallo *et al*, 1997). At low exposure doses ($VT = 100$ Vs) the resistance decrease was shown to be a nonlinear function of pulse train frequency, whereas at $VT = 300$ Vs no frequency dependence was seen. Permeabilization of the SC appears to be due to pore formation by electric pulses, and recovery to pore resealing (Benz and Zimmerman, 1981; Pliquett *et al*, 1995). We expect the resealing time to be determined by pore size and resilience of the lipid bilayers that make up the bulk of the SC. The plateau value of 30–50 Hz for a long-term resistance drop implies that the recovery time of the SC is in the range of 20–33 ms. If a second pulse is delivered within this time, a cumulative poration effect may be achieved, resulting in permanent permeability changes. The steep increase of MB transport observed at >60 Hz could be due to rapid delivery of consecutive pulses within <20 ms, resulting in a cumulative effect (e.g., heating) that produces severe skin damage. To minimize adverse skin effects, the majority of our pulsing was carried out at 40 Hz.

Skin resistance recovers rapidly after each pulse as long as the cumulative dose is kept below a threshold value (Gallo *et al*, 1997). Permeabilization becomes long-term only after the skin has experienced

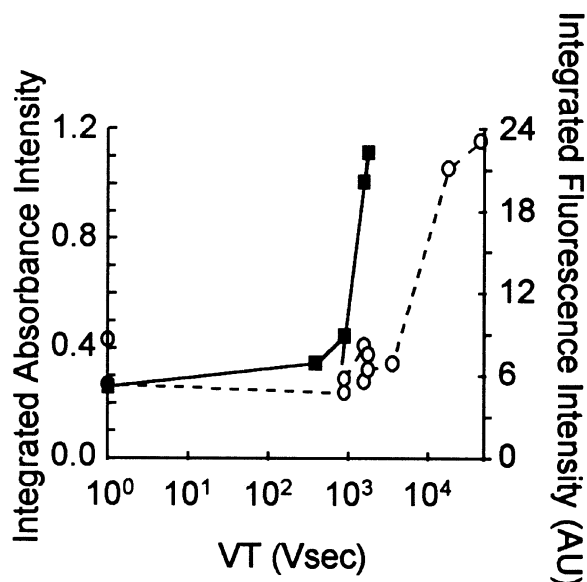


Figure 5. Total penetration of MB in biopsy sections as a function of $\log VT$ (Vs). Penetration as measured by the integrated intensity (area under the curve) from image analyses of fluorescence (■) and light transmittance (○).

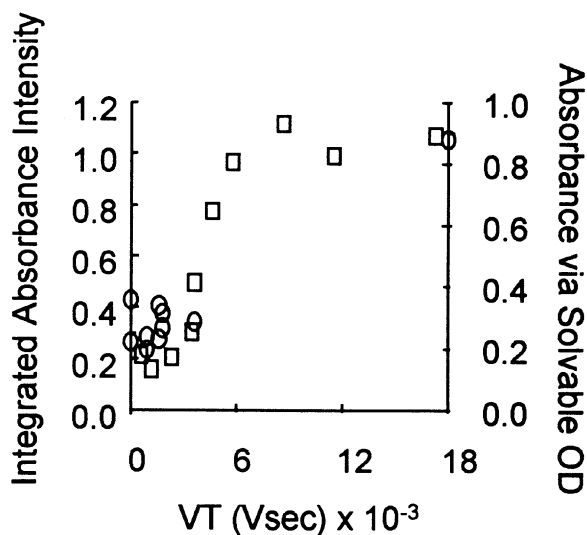


Figure 6. Total amount of MB penetration as a function of electrical exposure dose VT , as determined by the concentration (via absorbance) in Solvable supernatant (□) and light transmittance of scanned images (○).

a sufficiently high exposure dose. Above this threshold the skin is permeable for a time even after pulsing ceases. This implies that long-term openings or pores are created. This hypothesis is supported by our observation that enhanced MB penetration was seen when applied to the skin after pulsing at an above-threshold dose (Table I).

Taken together, our results support the view (Bommannan *et al*, 1994; Chizmadzhev *et al*, 1995) that, under these conditions, molecular transport takes place through a combination of forces. An initial permeabilization (electroporation) is required for transport to begin; above that threshold, continued pulsing results in enhanced transport, probably due to electromotive forces (electrophoresis and electro-osmosis). The importance of electroporation as a factor in this process is emphasized by the relatively poor penetration by iontophoresis alone. Furthermore, transport cannot be attributed to “high voltage

iontophoresis" (i.e., electromotive processes) alone, because penetration of MB, applied to the skin only after pulsing, was enhanced due to diffusion of the drug through persisting electropores (Table I). We are now carrying out additional experiments using various physical techniques to characterize the long-term response of skin to electric fields.

In some ways comparing our results with others is problematic. Prausnitz *et al* (1993) report that transdermal delivery of calcein, a tetraanionic molecule (molecular weight 623), is enhanced in an *in vivo* system using hairless rats. In their system, however, the equivalent electric dose was about 280 Vs, and plasma levels were detected 30–60 min after pulsing, reflecting systemic delivery ($\approx 10 \mu\text{g}$ per cm^2 per h) via the blood supply at the epidermal–dermal boundary. Riviere *et al* (1995) monitored the transport of luteinizing hormone releasing hormone (molecular weight 1182) using a perfused porcine skin flap and iontophoresis enhanced by 1–3 electroporative pulses. Delivery of this cationic drug ($2 \mu\text{g}$ per cm^2 per h) was also assayed by measuring the amount present in the vasculature. Topical drug administration can be used for systemic delivery via the circulatory system or for localized delivery (e.g., to the skin). The relative importance of transport into or through the skin depends on the desired target. For example, if insulin delivery is the goal, transcutaneous delivery would be necessary. Because our interest at this time is primarily in delivery of drugs for cutaneous photodynamic therapy, controlled delivery to the skin is more desirable.

Furthermore, the bulk of work in the field of electroporation-enhanced drug delivery uses diffusion chambers and heat-stripped or dermatomed skin, and measures the amount of material traversing the skin sample. We use intact full-thickness tissue with both electrodes located on the SC surface, and monitor delivery to the skin, measuring both the amount in the sample and the penetration depth. We believe that our system more closely models any projected *in vivo* use; however, a comparison of our results with some studies using a chamber apparatus is informative. For example, Vanbever and Pr eat (1995) reported transport of the cationic metoprolol (molecular weight 267) of up to $500 \mu\text{g}$ per cm^2 per h with five pulses of 250 V and $\tau = 620$ ms ($VT = 775$ Vs), using a hairless rat skin (full-thickness) model. Prausnitz *et al* (1995) saw enhanced flux of heparin (anionic, 5–30 KD) up to $500 \mu\text{g}$ per cm^2 per h using heat-stripped human cadaver skin. In that instance, $>43,000$ pulses (150–350 V, $\tau = 1.9$ ms, 12 Hz, $VT > 28,000$ Vs) were applied. Thus when electric pulse doses approximated those used in this work, molecular flux was within an order of magnitude of the values we report for MB. In most cases, however, electric pulse doses used in previous studies were considerably less than those reported herein.

Some adverse side-effects of electrically enhanced transdermal transport are possible, and may include such events as pain sensation, burns, local skin irritation, or sensitization reactions. Electric current applied to the skin, however, is routinely used in a wide range of applications, including iontophoresis, transcutaneous electrical nerve stimulation, electromyography, and enhancement of wound and bone fracture healing. Consequently there is an extensive body of literature dealing with the biologic effects of electric current (Ledger, 1992; Prausnitz, 1996; Lee, 1997). Judicious selection of various parameters, including voltage or current, pulse length, pulse frequency, and treatment duration, must be used to minimize any adverse effects while maintaining efficacy.

As previously mentioned, this work was initiated with the goal of improving local delivery of photosensitizers. One of the major drawbacks to the use of FDA-approved Photofrin in photodynamic therapy is long-term (≥ 30 d) patient photosensitivity (Dougherty and Marcus, 1992) as a consequence of its systemic administration. The tissue levels achieved with electric pulse enhanced delivery, 0.05–0.3 mg per gram of tissue (Table I), are orders of magnitude greater than the levels achieved 24 h after intravenous or intraperitoneal injection of various hydrophilic porphyrin photosensitizers (Boyle and Dolphin, 1996). Furthermore, with systemic drug delivery only about 0.1% of the drug dose reaches the target area (Boyle and Dolphin, 1996); with pulsed electric-field delivery virtually all of the drug is delivered to the target

region, it is delivered more quickly, and systemic toxicity and/or metabolism is reduced.

We think that electroporation will have important applications in the field of drug delivery, and we are continuing studies to optimize the parameters for electric pulse enhanced transport. We suggest that this system may serve as a model for electroenhanced epidermal or transdermal transport in a variety of fields where topical drug delivery is a goal.

We gratefully acknowledge the assistance of James E. Whitaker of the Department of Dermatology for his help with the absorbance and fluorescence imaging, of Dr. Richard Cheney of the Pathology Department for his helpful discussions regarding our histologic observations, and of Dr. John Canty of the Department of Medicine at SUNY/UB who supplied much of the porcine skin used in this project. This work is supported in part by a grant from the Roswell Park Alliance Foundation, and grants RO1 GM 30969 (to Dr. Sek Wen Hui) and 5PO1 CA 55791 (to Dr. Allan R. Oseroff) from the National Institutes of Health. Stephen A. Gallo was supported by a training grant fellowship 5T32CA61800 from the National Cancer Institute.

REFERENCES

- Bellnier DA, Greco WR, Parsons JC, Oseroff AR, Kuebler A, Dougherty TJ: An assay for the quantitation of Photofrin in tissues and fluids. *Photochem Photobiol* 66:237–244, 1997
- Benz R, Zimmermann U: The resealing process of lipid bilayers after reversible electrical breakdown. *Biochimica et Biophysica Acta* 640:169–178, 1981
- Berti JJ, Lipsky JJ: Transcutaneous drug delivery: a practical review. *Mayo Clin Proc* 70: 581–586, 1995
- Bomann DB, Tamada J, Leung L, Potts RO: Effect of electroporation on transdermal iontophoretic delivery of luteinizing hormone releasing hormone (LHRH) in vitro. *Pharm Res* 11:1809–1814, 1994
- Boyle RW, Dolphin D: Structure and biodistribution relationships of photodynamic sensitizers. *Photochem Photobiol* 64:469–485, 1996
- Bronaugh RL, Stewart RF, Congdon ER: Methods for in vitro percutaneous absorption studies. II. Animal models for human skin. *Toxicol Appl Pharm* 62:481–488, 1982
- Chang DC: Structure and dynamics of electric field-induced membrane pores as revealed by rapid-freezing electron microscopy. In: Chang DC, Chassy BM, Saunders JA, Sowers AE (eds). *Guide to Electroporation and Electrofusion*. San Diego: Academic Press, 1992, pp. 9–27
- Chizmadzhev YA, Zarnitsin VG, Weaver JC, Potts RO: Mechanism of electroinduced ionic species transport through a multilamellar lipid system. *Biophys J* 68: 749–765, 1995
- Chizmadzhev YA, Indenbom AV, Kuzmin PI, Galichenko SV, Weaver JC, Potts RO: Electrical properties of skin at moderate voltages: contribution of appendageal macropores. *Biophys J* 74:843–856, 1998
- Dougherty TJ, Marcus SL: Photodynamic therapy. *Eur J Cancer* 28A:1734–1742, 1992
- Edwards DA, Langer R: A linear theory of transdermal transport phenomena. *J Pharm Sci* 83:1315–1334, 1994
- Edwards DA, Prausnitz MR, Langer R, Weaver JC: Analysis of enhanced transdermal transport by skin electroporation. *J Controlled Release* 34:211–221, 1995
- Ferry LL, Argentieri G, Lochner DH: The comparative histology of porcine and guinea pig skin with respect to iontophoretic drug delivery. *Pharm Acta Helv* 70:43–56, 1995
- Gallo SA, Oseroff AR, Johnson PG, Hui SW: Characterization of electric-pulse-induced permeabilization of porcine skin using surface electrodes. *Biophys J* 72: 2805–2811, 1997
- Hofmann GA, Rustrum WV, Suder KS: Electro-incorporation of microcarriers as a method for the transdermal delivery of large molecules. *Bioelectrochem Bioenergetics* 38:209–222, 1995
- Jacques SL, McAuliffe DJ, Blank IH, Parrish JA: Controlled removal of human stratum corneum by pulsed laser. *J Invest Dermatol* 88:88–93, 1987
- Ledger PW: Skin biological issues in electrically enhanced transdermal delivery. *Advanced Drug Delivery Rev* 9:289–307, 1992
- Lee RC: Injury by electrical forces. *Current Problems Surg* 34:677–764, 1997
- Lee RD, White HS, Scott ER: Visualization of iontophoretic transport paths in cultured and animal skin models. *J Pharm Sci* 85:1186–1190, 1996
- Liang H, Purucker WJ, Stenger DA, Kubiniec RT, Hui SW: Uptake of fluorescence-labeled dextrans by 10T 1/2 fibroblasts following permeation by rectangular and exponential-decay electric field pulses. *Bioteniques* 6:550–558, 1988
- Lilge L, O'Carroll C, Wilson BC: A solubilization technique for photosensitizer quantification in ex vivo tissue samples. *J Photochem Photobiol B* 39:229–235, 1997
- Mir LM, Orlovski S, Belehradec J, *et al*: Biomedical applications of electric pulses with special emphasis on antitumor electrochemotherapy. *Bioelectrochem Bioenergetics* 38:203–207, 1995
- Pliquet U, Langer R, Weaver JC: Changes in the passive electrical properties of human stratum corneum due to electroporation. *Biochimica et Biophysica Acta* 1239: 111–121, 1995
- Pliquet UF, Zewert TE, Chen T, Langer R, Weaver JC: Imaging of fluorescent molecule and small ion transport through human stratum corneum during high voltage pulsing – localized transport regions are involved. *Biophys Chem* 58:185–204, 1996

- Prausnitz MR: The effects of electric current applied to the skin: a review for transdermal drug delivery. *Advanced Drug Delivery Rev* 18:395–425, 1996
- Prausnitz MR, Bose VG, Langer R, Weaver JC: Electroporation of mammalian skin: a mechanism to enhance transdermal drug delivery. *Proc Natl Acad Sci USA* 90:10504–10508, 1993
- Prausnitz MR, Edelman ER, Gimm JA, Langer R, Weaver JC: Transdermal delivery of heparin by skin electroporation. *Bio-Technology* 13:1205–1209, 1995
- Riviere JE, Monteiro-Riviere NA: The isolated perfused porcine skin flap as an in vitro model for percutaneous absorption and cutaneous toxicology. *Crit Rev Toxicol* 21:329–344, 1991
- Riviere JE, Monteiro-Riviere NA, Rogers RA, Bommannan D, Tamada JA, Potts RO: Pulsatile transdermal delivery of LHRH using electroporation – drug delivery and skin toxicology. *J Controlled Release* 36:229–233, 1995
- Scheuplein RJ, Bronaugh RL: Percutaneous absorption. In: Goldsmith LA (ed.) *Biochemistry and Physiology of the Skin*. New York: Oxford University Press, 1983, pp. 1255–1295
- Singh S, Singh J: Transdermal drug delivery by passive diffusion and iontophoresis: a review. *Med Res Rev* 13:569–621, 1993
- Steinstrasser I, Merkle HP: Dermal metabolism of topically applied drugs: pathways and models reconsidered. *Pharm Acta Helv* 70:3–24, 1995
- Titomirov AV, Sukharev S, Kistanova E: In vivo electroporation and stable transformation of skin cells of newborn mice by plasmid DNA. *Biochim Biophys Acta* 1088:131–134, 1991
- Tuite EM, Kelly JM: Photochemical interactions of methylene blue and analogues with DNA and other biological substrates. *J Photochem Photobiol B Biol* 21:103–124, 1993
- Vanbever R, Pr at V: Factors affecting transdermal delivery of metoprolol by electroporation. *Bioelectrochem Bioenergetics* 38:223–228, 1995